Eye (2021) 35:959–965
https://doi.org/10.1038/s41433-020-1006-x

The ROYAL COLLEGE of OPHTHALMOLOGISTS

ARTICLE

The agreement between optical coherence tomography angiography and non-mydriatic retinal camera in estimating the optic nerve head parameters and relations with the peripapillary vessel density in primary open-angle glaucoma

Mehmet Talay Koylu[1] · Hayati Yilmaz[2] · Alper Can Yilmaz[1]

Received: 9 February 2020 / Revised: 18 May 2020 / Accepted: 26 May 2020 / Published online: 4 June 2020

Abstract

Background/objectives To investigate the agreement between optical coherence tomography angiography (OCT-A) and non-mydriatic retinal camera (NMRC) in estimating the optic nerve head (ONH) parameters and evaluate the associations between peripapillary vessel density (VD) with ONH parameters assessed by both devices.

Methods The OCT-A and NMRC images of 262 participants (138 eyes were diagnosed with POAG, 63 were glaucoma suspect, and 61 were healthy subjects) were screened retrospectively. The vertical cup-to-disc ratio (VCDR), cup-to-disc area ratio (CDAR), rim area (RA), disc area (DA), and cup volume (CV) were recorded using both devices. Peripapillary VD data were also recorded using OCT-A. The intraclass correlation coefficient (ICC) and Bland–Altman plots were obtained to investigate the agreement between the devices. Age- and intraocular pressure (IOP)-corrected associations between the VD and ONH parameters measured by the two devices were analyzed using linear regression models.

Results ICC revealed excellent agreement for VCDR and CDAR, but poor agreement for RA, DA, and CV (ICC = 0.801, 0.793, 0.445, 0.298, and 0.527, respectively). The Bland–Altman plots showed poor agreement for VCDR and CDAR with a large span of limits of agreement (0.500 and 0.528, respectively) and significant proportional biases ($P < 0.05$). VD was found to be strongly associated with the VCDR and CDAR measurements of both devices ($P < 0.001$), but the associations were stronger for the measurements of NMRC.

Conclusions The disagreement between the devices should be considered in clinical practice. The associations between the VD and ONH parameters proved once again the importance of the ONH parameters in terms of the management of glaucoma patients.

Introduction

The diagnosis of open-angle glaucoma is based on intraocular pressure (IOP), optic nerve head (ONH) parameters, and visual field (VF) analysis. The investigation of ONH is an important part of glaucoma diagnosis and management [1]. Estimating the cup-to-disc ratio (CDR) is one of the reference parameters for diagnosing glaucoma and is also a main indicator for assessing glaucomatous changes over time [2, 3]. Therefore, it is essential to carefully document CDR. Non-mydriatic retinal camera (NMRC) is a helpful tool for evaluating ONH parameters [4]. However, evaluating CDR using slit-lamp biomicroscopy and stereoscopic photography remains subjective with moderate to high intra- and inter-observer variability [5, 6].

Optical coherence tomography angiography (OCT-A), as an extension of the OCT, allows measuring and quantifying the macular and peripapillary areas, and provides vessel densities along with structural information. It is well established with previous studies that OCT-A has excellent repeatability and reproducibility [7–10]. In addition, the reduction of the vessel density (VD) and blood-flow index in

✉ Mehmet Talay Koylu
talaykoylu@hotmail.com

✉ Hayati Yilmaz
dr.hyilmaz@hotmail.com

[1] Department of Ophthalmology, Gulhane Medical Faculty, Health Sciences University, Ankara, Turkey

[2] Department of Ophthalmology, Umraniye Training and Research Hospital, Health Sciences University, Istanbul, Turkey

glaucomatous eye is well documented by numerous studies [11, 12]. The aim of this study was to compare the morphologic findings of ONH including CDR measured by NMRC with OCT-A and their associations with peripapillary VD.

Materials and methods

The data obtained from the present study were acquired with the approval of the Institutional Clinical Research Ethics Committee of Health Sciences University, Gulhane Medical Faculty, and the study was completed in agreement with the principles of the Declaration of Helsinki. The study was designed retrospectively. Patients with a diagnosis of primary open-angle glaucoma (POAG), glaucoma suspect (GS), or healthy subjects (HS) that presented to our glaucoma clinics between 2018 and 2019 and had complete ophthalmological examination including visual acuity, intraocular pressure, slit-lamp biomicroscopy, and non-dilated fundoscopy along with the VF testing (Humprey Field Analyzer II, Carl Zeiss Meditec, Inc), OCT scans of the RNFL (Spectralis, Heidelberg Engineering, Heidelberg, Germany), OCT-A scans (Angiovue, Optovue Inc., Fremont, CA, USA), and NMRC (Nonmyd WX; Kowa Optimed Inc., Japan) images at the same visit were screened. The diagnosis of the POAG and GS were made in accordance with the European Glaucoma Society's Terminology and Guidelines for Glaucoma textbook [1]. Increased IOP (>21 mmHg), presence of acquired characteristic glaucomatous changes of the ONH, presence of glaucomatous VF defect, and open angle were the features of the POAG. GS diagnosis was made with the presence of at least one suspicious changes in VF, ONH, and RNFL, and with normal or increased IOP. The exclusion criteria were age under 18 years, refractive error of >±3 diopters, presence of any other ophthalmological pathology that could confound the assessment results (e.g., diabetic or hypertensive retinal diseases, amblyopia, optic nerve anomalies, optic neuropathies other than POAG, and age-related macular degeneration), OCT-A signal strength of <70, and poor NMRC quality.

NMRC imaging

ONH was photographed twice by a glaucoma expert (MTK) and analyzed by two glaucoma experts (MTK and ACY) who were blinded to the patients' clinical data and OCT-A scans. Kowa 3D NMRC (Nonmyd WX; Kowa Optimed Inc., Japan), which is the stereoscopic fundus camera was used to take non-mydriatic fundus stereographs and both right and left parallactic images simultaneously through a single optical system handling light paths in two directions. [13] Kowa 3D NMRC can display a depth map, which shows the depth of the disc separated by color, a 3D display of the optic disc, diagnostic parameters. In accordance with the algorithm provided by Kowa Optimed Inc., all measurements were conducted after correcting for magnification by refractive error, axial length, and corneal curvature. After photographs were taken, two images with binocular parallax were obtained then, two images were automatically superimposed on the monitor by built-in software, and a stereoscopic 3D image was generated using polarized 3D glasses. The examiner stereoscopically observed the outline of the optic disc displayed on a monitor. The edge of disc is plotted using a computer mouse, and the cup is selected in a similar way, to determine their extent. After that, all other analysis was automatically performed by built-in software. The vertical CDR (VCDR), cup area to disc area ratio (CDAR), rim area (RA), disc area (DA), and cup volume (CV) values were recorded for both photographs after the images were analyzed.

The patients were divided into three groups according to the DA measurement of NMRC: small (area < 1.6 mm^2), medium (area = 1.6–2.0 mm^2), and large (area > 2.0 mm^2) optic discs. [14]

OCT-A ONH scanning

OCT-A scans were obtained using an AngioVue OCT-A system (Optovue Inc., Fremont, CA, USA). This device has an A-scan rate of 70,000/s using a light source of 840 nm. En face images were acquired focusing the ONH (4.5 × 4.5 mm) using the Angio Disc QuickVue module. Each scan consisted of 400 × 400 A-scans with two following B-scans at each fixed location. To reduce motion artifacts, each scan comprised one orthogonal horizontal and vertical scan.

The device provides data on anatomic Bruch membrane opening (BMO)-based neuroretinal rim and ONH, retinal nerve fiber layer thickness (RNFLT), and peripapillary VD in a single scan. After scanning, VCDR, CDAR, RA, DA, and CV values along with the small VD of the whole retinal peripapillary capillary plexus (RPCP) were recorded.

Statistical analyses

Quantitative variables were described as mean and standard deviation, and qualitative variables as percentages. The test-retest variability of the two NMRC photographs of each subject was calculated using the Kappa measure of agreement method. The paired *t*-test was used to compare the results obtained from the two devices. The magnitude of the disagreement between the two raters of NMRC images and between the NMRC and OCT-A data was estimated as the mean absolute differences in the VCDR, CDAR, RA, DA, and CV values. The inter-rater variability of the NMRC and the agreement between the corresponding NMRC and

Table 1 Demographic and clinical data of the study subjects.

	POAG patients	GS	HS	*P*
Age (y. ± SD)	60.1 ± 19.2	58.9 ± 18.5	59.5 ± 18.8	0.721
Female (*n*/%)	78/56.5	36/57.1	35/57.3	0.542
BCVA (LogMAR ± SD)	0.73 ± 0.32[a]	0.00 ± 0.00	0.00 ± 0.00	**<0.001**
IOP (mmHg ± SD)	15.2 ± 6.4	14.3 ± 4.3	14.1 ± 3.7	0.254
VF (MD ± SD)	−4.18 ± 3.12[a]	−0.12 ± 2.7	0.21 ± 1.4	**<0.001**

The significant *P* values expressed with bold style.

POAG primary open-angle glaucoma, *GS* glaucoma suspect, *HS* healthy subjects, *SD* standard deviation, *BCVA* best corrected visual acuity, *IOP* intraocular pressure, *VF* visual field, *MD* mean deviation.

[a]The reason of the significance among groups.

Table 2 Mean values of the OCT-A and NMRC measurements of the ONH parameters.

	OCT-A	NMRC	*P*
VCDR (SD)	0.57 (0.17)	0.53 (0.13)	0.078
CDAR (SD)	0.31 (0.17)	0.30 (0.14)	0.988
RA, mm^2 (SD)	1.44 (0.46)	1.92 (0.49	**<0.001**
DA, mm^2 (SD)	2.03 (0.46)	2.81 (0.58)	**<0.001**
CV, mm^3 (SD)	0.16 (0.17)	0.32 (0.39)	**<0.001**

The significant *P* values expressed with bold style.

OCT-A optical coherence tomography angiography, *NMRC* non-mydriatic retinal camera, *VCDR* vertical cup-to-disc ratio, *CDA* cup-to-disc area ratio, *RA* rim area, *DA* disc area, *CV* cup volume.

OCT-A data was calculated with the intraclass coefficient (ICC) [15]. Absolute ICCs based on the mixed model analysis of variance were used in the present study. An ICC value of <0.4 was accepted to indicate poor agreement, 0.4–0.75 represented fair to good agreement, and a value of >0.75 indicated excellent agreement [14, 16]. The ICC calculations were executed before and after the subjects were classified as having small, medium, and large optic discs. The ICC calculations were also performed after the subjects were divided into POAG, GS, and HS groups. The Shapiro–Wilk test was used to determine whether the differences between the corresponding NMRC and OCT-A data were normally distributed. Bland–Altman plots were used to assess the agreement between NMRC and OCT-A in ONH parameters. One-sample *t*-test was performed for the differences before the Bland–Altman plots were created [17]. Linear regression analyses were undertaken to determine the significance of proportional biases. To analyze the associations of ONH parameters with the small VD of RPCP, after checking the collinearity, age- and IOP-corrected multiple regression models were created. The regression results revealed coefficients (B), 95% confidence interval, and *P* values. Statistical analyses were conducted using SPSS v. 21 (SPSS, Inc., Chicago, IL, USA). A *P* value of <0.05 was considered statistically significant.

Results

Of the 312 patients screened, 262 (57% female, mean age 59.4 ± 18.3 years) met the inclusion criteria, and only one eye of each patient (the one with better OCT-A quality) was enrolled for the statistical analysis. A total of 138 eyes were diagnosed with POAG, 63 had a GS, and 61 had no-glaucoma (HS). GSs consisted of 59 eyes with suspected ONH damages without VF and RNFL defects, and 4 with RNFL defect without VF defect and ONH changes. The demographic and clinical data of the subjects were given in Table 1.

Table 2 presents the mean VCDR, CDAR, DA, RA, and CV values of OCT-A and NMRC and the results of the paired *t*-test. The devices significantly differed from each other in terms of the DA, RA, and CV measurements ($P < 0.001$). The difference was the greatest for the CV measurement. The VCDR, CDAR, DA, RA, and CV measurements of the two devices were all positively correlated ($R = 0.711$, 0.734, 0.746, 0.445, and 0.262, respectively.) The correlations were weaker for RA and CV. In accordance with the paired *t*-test and Pearson's correlation test results no further statistical analyses were executed for the DA, RA, and CV measurements.

The overall mean value of the small VD of RPCP was 48.09%. This parameter was calculated as 46.06% for the subjects with a DA of <1.60 mm^2, 48.94% for 1.60–2.00 mm^2, and 48.12% for >2.00 mm^2. There was no significant difference according to the disc sizes ($P > 0.05$, ANOVA). The mean small VD values of RPCP of the POAG, GS, and HS were 46.18%, 51.01%, and 52.60%, respectively. The VD of POAG was significantly lower than that of GS ($P < 0.001$, post-hoc Tukey, ANOVA) and NG ($P < 0.001$, post-hoc Tukey, ANOVA). There was no significant difference between the GS and HS ($P = 0.674$, post-hoc Tukey, ANOVA).

Agreement between NMRC and OCT-A

The reliability of the measurements of two NMRC images was excellent ($\kappa = 0.902$ and $P = 0.764$ for the VCDR and $\kappa = 0.856$ and $P = 0.632$ for the CDAR). Excellent agreement in VCDR and CDAR estimates was observed between the two raters of the NMRC data (ICC = 0.891 for CDAR and 0.875 for CDAR). The results of ICC analyses are presented in Tables 3 and 4. There was an excellent agreement for the VCDR and CDAR measurements between the two devices (ICC = 0.801 and 0.793, respectively). The agreement was greater for the larger ONHs in

Table 3 Intraclass correlation coefficient (ICC) between OCT-A and NMRC.

	ICC	95% CI (lower/upper bounds)	*P*
VCDR			
Total	0.801	0.724/0.854	**<0.001**
<1.60 mm^2	0.709	0.538/0.817	**<0.001**
1.60–2.00 mm^2	0.785	0.532/0.901	**<0.001**
>2.00 mm^2	0.807	0.531/0.902	**<0.001**
CDAR			
Total	0.793	0.728/0.843	**<0.001**
<1.60 mm^2	0.648	0.443/0.778	**<0.001**
1.60–2.00 mm^2	0.688	0.333/0.855	**<0.001**
>2.00 mm^2	0.844	0.770/0.894	**<0.001**

The significant *P* values expressed with bold style.

OCT-A optical coherence tomography angiography, *NMRC* non-mydriatic retinal camera, *VCDR* vertical cup-to-disc ratio, *CDAR* cup-to-disc area ratio.

Table 4 Intraclass correlation coefficient (ICC) between OCT-A and NMRC.

	ICC	95% CI (lower/upper bounds)	*P*
VCDR			
POAG	0.764	0.566/0.880	**<0.001**
GS	0.678	0.528/0.779	**<0.001**
HS	0.431	0.027/0.672	**0.020**
CDAR			
POAG	0.770	0.546/0.884	**<0.001**
GS	0.656	0.508/0.760	**<0.001**
HS	0.511	0.149/0.721	**0.006**

The significant *P* values expressed with bold style.

OCT-A optical coherence tomography angiography, *NMRC* non-mydriatic retinal camera, *VCDR* vertical cup-to-disc ratio, *CDAR* cup-to-disc area ratio, *POAG* primer open-angle glaucoma, *GS* glaucoma suspect, *HS* healthy subjects.

all corresponding measured parameters (Table 3). The agreements were also greater for the POAG patients than GS and HS (Table 4).

Figure 1 presents the scatter plot of OCT-A against NMRC for VCDR and CDAR, as well as the Bland–Altman plots of these parameters. The one-sample *t*-test results were insignificant in relation to differences ($P = 0.193$ for the CDAR and 0.095 for the VCDR). The Bland–Altman plots showed the mean bias ± SD between the measurements of VCDR and CDAR assessed by OCT-A and NMRC as 0.038 ± 0.128 and -0.0001 ± 0.135, respectively. The limits of agreement (LOA) were −0.212–0.288 for VCDR, and −0.264–0.264 for CDAR. The slopes of the VCDR and CDAR regression lines were calculated as 0.30 and 0.31, respectively, indicating that OCT-A tended to produce higher rates than NMRC in larger VCDR and CDAR, and vice versa. The linear regression analyses of proportional bias were statistically significant ($P < 0.001$ for VCDR and $P = 0.012$ for CDAR). The wide spans of LOA (0.500 for VCDR and 0.564 for CDAR) and the statistically significant proportional biases suggested poor agreement between the two devices.

Associations with the VD of RPCP

In the multivariate analysis of the VD of global RPCP, we created a model in which we searched for the associations with the age, IOP, VCDR, and CDAR (of the OCT-A device). In this model, we excluded the CDAR due to collinearity with the VCDR, therefore, we created a similar model in which we included CDAR instead of VCDR. The results of these two regression models are given in Table 5. The VCDR and CDAR of OCT-A were found to be strongly associated with the small VD of RPCP ($B = -23.051$ for VCDR and -20.700 for CDAR).

Discussion

The evaluation of the ONH parameters is of paramount importance in glaucoma management [3, 18–21]. There are numerous methods to investigate the morphological findings of ONH to identify early glaucomatous changes [22]. Stereophototography has been widely used for decades and was once considered as a gold standard technique for this purpose. NMRC, which is a stereoscopic fundus camera used to take non-mydriatic fundus stereographs, can display a depth map that shows the depth of the disc separated by color, provides a 3D display of the optic disc, and automatically calculates diagnostic parameters [20, 23–26]. OCT-A, as an extension of the OCT technology, is relatively new in the ophthalmology practice and has recently started to be used at an increasing frequency in glaucoma management. Previous studies on OCT-A described reduction in VD and the flow index of ONH, peripapillary area, and macular region [12, 27–32]. In the present study, we first investigated the morphological findings of ONH using OCT-A and NMRC, and then compared the results obtained from these two devices. Secondly, we explored the associations between peripapillary VD based on the ONH parameters assessed by these methods.

The agreement between OCT-A and NMRC was found to be poor in the present study. Even though ICC revealed excellent agreement between NMRC and OCT-A in terms of VCDR and CDAR (ICC = 0.801 and 0.793, respectively), the Bland–Altman plots showed poor agreement with a wide span of LOA (0.500 and 0.528, respectively) and statistically significant proportional bias values. Our results were similar with the previous studies which investigated the agreement between OCT and stereoscopic

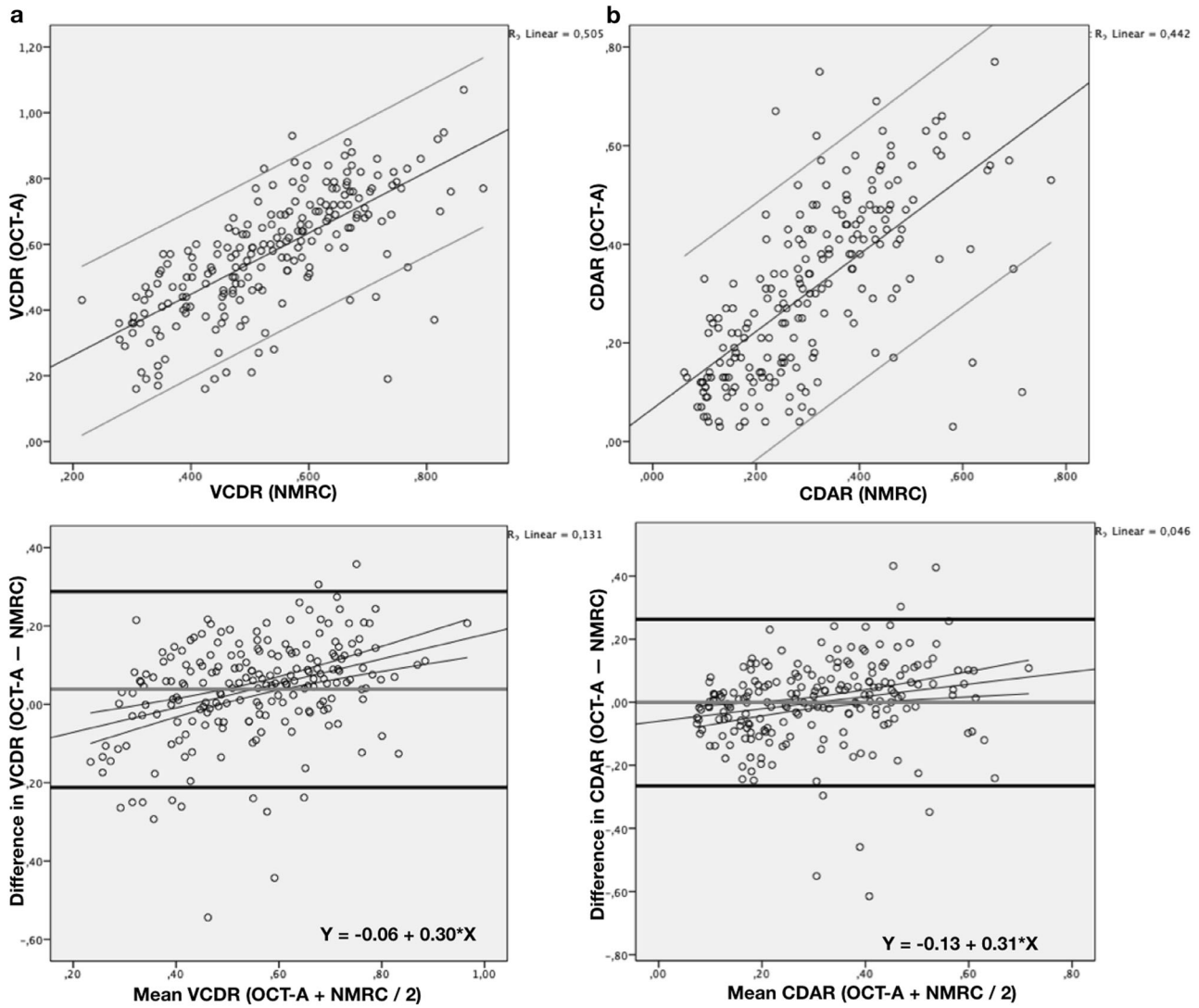

Fig. 1 The scatter and Bland-Altman plots of the study subjects. Scatter plot of OCT-A against NMRC for VCDR (column **a**, top) and CDAR (column **b**, top) and the Bland–Altman plots for the agreement between OCT-A and NMRC for the VCDR (column **a**, bottom) and CDAR (column **b**, bottom). Scatter plots were given with the regression line and the 95% limits of agreements Bland–Altman plots were given with the mean of the difference, 1.96 SDs, and the regression lines. OCT-A optical coherence tomography angiography, NMRC non-mydriatic retinal camera, VCDR vertical cup-to-disc ratio, CDAR cup-to-disc area ratio, SD standard deviation.

photography [14, 33]. In addition, we investigate whether there was any agreement between the two devices in terms of RA, DA, and CV; however, we found the agreement to be poor even in relation to VCDR and CDAR. Chan et al. compared three different devices: OCT, Heidelberg retina tomography (HRT), and stereoscopic photography. They reported that the disagreement in the CDR measurements between these modalities altered the five-year risk estimation of glaucoma progression in untreated ocular hypertension eyes [33]. Chan showed the importance of the same device we used for the management of GSs, emphasizing that it could alter treatment decision. Mwanza et al. also determined that OCT and stereoscopic photography had disagreement concerning the horizontal and vertical CDR measurements [14]. Both Chan's and Mwanza's studies suggest that the cause of this disagreement could be related to the different disc margin determination, and the assessment of ONH in stereoscopic photography relies on defining the visible disc margin by an expert; on the other hand, the OCT devices they used in their studies, similar to our OCT-A device, recognize BMO, which is accepted as the true anatomical outer border of the neuroretinal rim as the disc margin. Reis et al. also described that the disc margin detected on photographs fell outside BMO in all sectors but the inferotemporal sector where the opposite situation was observed. Also the fact that the RA and CV measurements differ between two devices means that the delineation of the cup and the margin between the cup and rim is different.

Table 5 The linear regression models for the RPCP small VD.

	B	95% CI (lower/upper bounds)	*P*
Model 1 ($R^2 = 0.287$)			
Age	−0.139	−0.208/0.070	**<0.001**
IOP	0.182	−0.130/0.494	0.356
VCDR (OCT-A)	−23.051	−28.925/−17.178	**<0.001**
Model 2 ($R^2 = 0.257$)			
Age	−0.148	−0.218/0.078	**<0.001**
IOP	0.223	−0.096/0.541	0.170
CDAR (OCT-A)	−20.700	−26.507/−14.893	**<0.001**

The significant *P* values expressed with bold style.

RPCP retinal peripapillary capillary plexus, *VD* vessel density, *B* coefficient, *CI* confidence interval, *IOP* intraocular pressure, *VCDR* vertical cup-to-disc ratio, *OCT-A* optical coherence tomography angiography, CDAR cup-to-disc area ratio.

This proves that selecting different algorithms that determines the disc margin, visible or BMO based, would alter all ONH parameters calculations.

The analyses of ICC revealed that disc size was very important for the agreement between the devices. The agreement was inferior in smaller optic discs and better for the larger ones. Jayasundera et al. and Correnti et al. reported similar results in their comparison of HRT, stereoscopic photography, and digital stereoscopic optic disc camera [34, 35]. This could be the reason why the agreement between the two devices in terms of the VCDR and CDAR measurements was better for the POAG patients than GSs and HS.

The main and most important outcome of this study was that the ONH parameters assessed by OCT-A were found to be closely related to the peripapillary VD independent of age and IOP. Enders et al. investigated the association between the ONH parameters assessed by OCT with VD, and they also found out that CDR and VD were strongly and negatively correlated [36].

The first limitation of this study is that comparing ONH parameters between NMRC and OCT-A could cause potential bias because only the OCT-A could calculate the BMO-based neuroretinal rim, however we performed this study because we also aimed to investigate the relation of peripapillary VD with ONH parameters, which is calculated with different algorithms. In this study we found associations between the VD and the ONH parameters, but it is also essential to search for the associations of the VF changes with the vessel densities. Lastly, using sectoral VD data and stratifying patients into subgroups in accordance with the severity of the glaucoma should be kept in mind while planning future studies in this matter.

In conclusion, in this retrospective study, we found that there was disagreement between NMRC and OCT-A in terms of the ONH measurements, including VCDR and CDAR. The agreement was better in larger disc sizes and patients with POAG. The measurements of the ONH parameters obtained from OCT-A were closely related to the peripapillary VD. Future prospective follow-up studies are needed to provide a better understanding of the alterations of VD through the changes in ONH parameters, which could be detected by NMRC and OCT-A.

Summary

What was known before

- OCT-A is a new technology for the assessment of the VD and in glaucoma, OCT-A is very helpful to manage the patients.

What this study adds

- OCT-A could also give reliable information about the ONH parameters. But the data of the different devices such as NMRC should not be used interchangeably.

Compliance with ethical standards

Conflict of interest The authors declare that they have no conflict of interest.

References

1. European Glaucoma Society terminology and guidelines for glaucoma, 4th edition—chapter 2: classification and terminology supported by EGS Foundation. Br J Ophthalmol. 2017;101:73–127. https://bjo.bmj.com/content/101/5/73.citation-tools.
2. Joshi PL, Jha B, Paudyal I, Thapa SS. Referral parameters for diagnosis of glaucoma in general eye clinic at Tilganga Institute of Ophthalmology. Nepal J Ophthalmol. 2019;11:33–9.
3. Jonas JB, Budde WM, Panda-Jonas S. Ophthalmoscopic evaluation of the optic nerve head. Surv Ophthalmol. 1999;43:293–320.
4. Koylu MT, Akincioglu D, Gokce G, Ozge G, Mumcuoglu T. Comparison of optic nerve head parameters measured by Kowa three dimensional non-mydriatic retinal camera and heidelberg retinal tomograph iii in healthy subjects. J Glaucoma-Cataract. 2019;14:180–6.
5. Jampel HD, Friedman D, Quigley H, Vitale S, Miller R, Knezevich F, et al. Agreement among glaucoma specialists in assessing progressive disc changes from photographs in open-angle glaucoma patients. Am J Ophthalmol. 2009;147:39–44.e1.
6. Tielsch JM, Katz J, Quigley HA, Miller NR, Sommer A. Intraobserver and interobserver agreement in measurement of optic disc characteristics. Ophthalmology. 1988;95:350–6.
7. Carpineto P, Mastropasqua R, Marchini G, Toto L, Di Nicola M, Di Antonio L. Reproducibility and repeatability of foveal avascular zone measurements in healthy subjects by optical coherence tomography angiography. Br J Ophthalmol. 2016;100:671–6.

8. Coscas F, Sellam A, Glacet-Bernard A, Jung C, Goudot M, Miere A, et al. Normative data for vascular density in superficial and deep capillary plexuses of healthy adults assessed by optical coherence tomography angiography. Investig Ophthalmol Vis Sci. 2016;57:OCT211–23.
9. Lupidi M, Coscas F, Cagini C, Fiore T, Spaccini E, Fruttini D, et al. Automated quantitative analysis of retinal microvasculature in normal eyes on optical coherence tomography angiography. Am J Ophthalmol. 2016;169:9–23.
10. Al-Sheikh M, Tepelus TC, Nazikyan T, Sadda SVR. Repeatability of automated vessel density measurements using optical coherence tomography angiography. Br J Ophthalmol. 2017;101:449–52.
11. Bojikian KD, Chen PP, Wen JC. Optical coherence tomography angiography in glaucoma. Curr Opin Ophthalmol. 2019;30:110–6.
12. Yarmohammadi A, Zangwill LM, Diniz-Filho A, Suh MH, Manalastas PI, Fatehee N, et al. Optical coherence tomography angiography vessel density in healthy, glaucoma suspect, and glaucoma eyes. Investig Ophthalmol Vis Sci. 2016;57:OCT451–9.
13. Asakawa K, Kato S, Shoji N, Morita T, Shimizu K. Evaluation of optic nerve head using a newly developed stereo retinal imaging technique by glaucoma specialist and non-expert-certified orthoptist. J Glaucoma. 2013;22:698–706.
14. Mwanza JC, Huang LY, Budenz DL, Shi W, Huang G, Lee RK. Differences in optical coherence tomography assessment of bruch membrane opening compared to stereoscopic photography for estimating cup-to-disc ratio. Am J Ophthalmol. 2017;184:34–41.
15. Hills M, Fleiss JL. The design and analysis of clinical experiments. J R Stat Soc Ser A. 1987;150:400.
16. Everitt BS, Fleiss JL. Statistical methods for rates and proportions. Biometrics. 1981;37:867.
17. Doğan NÖ. Bland-Altman analysis: a paradigm to understand correlation and agreement. Turk J Emerg Med. 2018;18:139–41.
18. Miglior S. Results of the European Glaucoma Prevention Study. Ophthalmology. 2005;112:366–75.
19. Gordon MO, Beiser JA, Brandt JD, Heuer DK, Higginbotham EJ, Johnson CA, et al. The Ocular Hypertension Treatment Study: baseline factors that predict the onset of primary open-angle glaucoma. Arch Ophthalmol. 2002;120:714–20.
20. Odberg T, Riise D. Early diagnosis of glaucoma: the value of successive stereophotography of the optic disc. Acta Ophthalmol. 1985;63:257–63.
21. Niyaz L, Yıldırım N, Musmul A. Optic nerve head parameters in a Turkish population over forty years of age. Turk J Ophthalmol. 2016;46:175–8.
22. Wollstein G, Garway-Heath DF, Fontana L, Hitchings RA. Identifying early glaucomatous changes: comparison between expert clinical assessment of optic disc photographs and confocal scanning ophthalmoscopy. Ophthalmology. 2000;107:2272–7.
23. Medeiros FA, Zangwill LM, Bowd C, Vasile C, Sample PA, Weinreb RN. Agreement between stereophotographic and confocal scanning laser ophthalmoscopy measurements of cup/disc ratio: effect on a predictive model for glaucoma development. J Glaucoma. 2007;16:209–14.
24. Pablo LE, Ferreras A, Fogagnolo P, Figus M, Pajarin AB. Optic nerve head changes in early glaucoma: a comparison between stereophotography and Heidelberg retina tomography. Eye. 2010;24:123–30.
25. Fogagnolo P, Romano S, Ranno S, Taibbi G, Pierrottet C, Ferreras A, et al. Diagnostic assessment of normal and pale optic nerve heads by confocal scanning laser ophthalmoscope and stereophotography. J Glaucoma. 2011;20:10–4.
26. Tatham AJ, Weinreb RN, Zangwill LM, Liebmann JM, Girkin CA, Medeiros FA. Estimated retinal ganglion cell counts in glaucomatous eyes with localized retinal nerve fiber layer defects. Am J Ophthalmol. 2013;156:578–87.e1.
27. Holló G. Relationship between optical coherence tomography sector peripapillary angioflowdensity and Octopus visual field cluster mean defect values. PLoS ONE. 2017;12:1–12.
28. Liu L, Jia Y, Takusagawa HL, Pechauer AD, Edmunds B, Lombardi L, et al. Optical coherence tomography angiography of the peripapillary retina in glaucoma. JAMA Ophthalmol. 2015;133:1045–52.
29. Jia Y, Wei E, Wang X, Zhang X, Morrison JC, Parikh M, et al. Optical coherence tomography angiography of optic disc perfusion in glaucoma. Ophthalmology. 2014;121:1322–32.
30. Bojikian KD, Chen PP, Wen JC. Optical coherence tomography angiography in glaucoma. Curr Opin Ophthalmol. 2019;30:110–6.
31. Yoshikawa Y, Shoji T, Kanno J, Kimura I, Hangai M, Shinoda K. Optic disc vessel density in nonglaucomatous and glaucomatous eyes: an enhanced-depth imaging optical coherence tomography angiography study. Clin Ophthalmol. 2018;12:1113–9.
32. Ang M, Tan ACS, Cheung CMG, Keane PA, Dolz-Marco R, Sng CCA, et al. Optical coherence tomography angiography: a review of current and future clinical applications. Graefe's Arch Clin Exp Ophthalmol. 2018;256:237–45.
33. Chan PP, Chiu V, Wong MO. Variability of vertical cup to disc ratio measurement and the effects of glaucoma 5-year risk estimation in untreated ocular hypertensive eyes. Br J Ophthalmol. 2019;103:361–8.
34. Jayasundera T, Danesh-Meyer HV, Donaldson M, Gamble G. Agreement between stereoscopic photographs, clinical assessment, Heidelberg retina tomograph and digital stereoscopic optic disc camera in estimating vertical cup:disc ratio. Clin Exp Ophthalmol. 2005;33:259–63.
35. Correnti AJ, Wollstein G, Price LL, Schuman JS. Comparison of optic nerve head assessment with a digital stereoscopic camera (Discam), scanning laser ophthalmoscopy, and stereophotography. Ophthalmology. 2003;110:1499–505.
36. Enders P, Longo V, Adler W, Horstmann J, Schaub F, Dietlein T. et al. Analysis of peripapillary vessel density and Bruch's membrane opening-based neuroretinal rim parameters in glaucoma using OCT and OCT-angiography. Eye. 2019;34:1086–93.